

Degradation in AlGaIn-based UV-C LEDs under constant current stress: A study on defect behaviors

Cite as: Appl. Phys. Lett. **116**, 203501 (2020); doi: [10.1063/5.0010540](https://doi.org/10.1063/5.0010540)

Submitted: 20 April 2020 · Accepted: 26 April 2020 ·

Published Online: 18 May 2020



View Online



Export Citation



CrossMark

Ying-Zhe Wang,¹ Xue-Feng Zheng,^{1,a)} Jia-Duo Zhu,^{1,a)} Lin-Lin Xu,² Sheng-Rui Xu,¹ Ren-Li Liang,² Jiang-Nan Dai,² Pei-Xian Li,³ Xiao-Wei Zhou,³ Wei Mao,¹ Jin-Cheng Zhang,¹ Xiao-Hua Ma,¹ and Yue Hao¹

AFFILIATIONS

¹Key Lab of Wide Bandgap Semiconductor Materials and Devices, School of Microelectronics, Xidian University, Xi'an 710071, People's Republic of China

²Wuhan National Laboratory for Optoelectronics, Huazhong University of Science and Technology, Wuhan 430074, People's Republic of China

³School of Advanced Materials and Nanotechnology, Xidian University, Xi'an 710071, People's Republic of China

^{a)}Authors to whom correspondence should be addressed: xfzheng@mail.xidian.edu.cn and jdzhu@xidian.edu.cn

ABSTRACT

Defect behaviors in the degradation of AlGaIn-based UV-C light emitting diodes (LEDs) under constant current stress have been intensively investigated in this work. It is found that both the reduction of the optical power and the increase in the leakage current are derived from the newly generated Ga vacancy (V_{Ga}) along dislocation, based on the evidence of a strong “yellow” emission peak at 515 nm in the photoluminescence spectra and an energy level of 0.25–0.38 eV. More importantly, the defect evolution behind it was determined through the deep level transient spectroscopy, secondary ion mass spectrometry measurements, and density functional theory. V_{Ga} is found to be generated by the departure of the unintentionally doped Mg from Mg_{Ga} along dislocation in the Si-doped region. The high activity of the unintentionally doped Mg under electrical stress can be an essential factor in the degradation of UV-C LEDs. This study not only provides an in-depth insight into the electrical stress-induced degradation in UV-C LEDs but also sheds light on the way for fabricating AlGaIn-based devices with high reliability.

Published under license by AIP Publishing. <https://doi.org/10.1063/5.0010540>

AlGaIn-based UV-C (210–280 nm) light emitting diodes (LEDs) have great potential in water/air/surface sterilization, medicine, biochemistry, and defense-related light sources, thanks to their small size, environment friendliness, and tunable emission wavelength.^{1–3} Nowadays, UV-C LEDs with a high output power^{4–6} and an external quantum efficiency (EQE)^{7–9} have been attained. However, it has been widely observed that the long-term operation can result in a significant degradation in their electrical and optical characteristics.^{10,11} Reliability problems have become one of the biggest obstacles to market competitiveness.

As for the degradation of optical characteristics, the reduction of optical power (OP) caused by electrical stress was usually attributed to the increase in the effective nonradiative recombination centers.^{12,13} For the degradation of electrical characteristics, most researchers suggested that the increased leakage current after stress can be ascribed to the generation of defects.^{14–16} All of these studies indicated the close relationship between defect generation and device performance

degradation. However, research on behaviors of defects in the degradation of AlGaIn-based UV-C LEDs is still limited to date, and essential questions such as where the defect is and how defect generates are also not clear. Therefore, an in-depth investigation on the nature of defects is pressing needed, which can effectively assist the device fabrication process to improve device reliability.

This work aims to explore defect behaviors in the degradation of UV-C LEDs during the constant current stress. The optical power, the reverse current, and the forward leakage current were evaluated by using the electroluminescence (EL) and current–voltage (I – V) measurements, respectively. Combined with the photoluminescence (PL) spectrum, the deep level transient spectroscopy (DLTS) measurement, the point-by-point correction secondary ion mass spectrometry (PCOR-SIMS), and the density functional theory (DFT), the behaviors of defect were characterized comprehensively. The correlation between defect behaviors and device degradation was also established.

The analysis was performed on a group of UV-C LEDs with a peak emission wavelength of 272 nm from the same wafer. The structures were prepared by the metal–organic chemical vapor deposition (MOCVD) on the sapphire substrate. The growth started with an AlN template, an $i\text{-Al}_{0.6}\text{Ga}_{0.4}\text{N}$ epilayer, and a Si-doped $n\text{-Al}_{0.6}\text{Ga}_{0.4}\text{N}$ buffer layer. The Si-doped active region consisted of six Si-doped $\text{Al}_{0.45}\text{Ga}_{0.55}\text{N}$ (2 nm)/ $\text{Al}_{0.57}\text{Ga}_{0.43}\text{N}$ (12 nm) multiple quantum wells (MQWs). A Mg-doped $p\text{-Al}_{0.8}\text{Ga}_{0.2}\text{N}$ with a thickness of 60 nm was used as an electron blocking layer (EBL), and a 280 nm $p\text{-GaN}$ film served as a p-type top layer. Finally, Ti/Al was used as an n-Ohmic contact layer, and Ni/Au was used as a p-Ohmic layer. Single chips were flip-chip mounted, and the chip size is $508\text{ }\mu\text{m} \times 203.2\text{ }\mu\text{m}$. UV-C LEDs were stressed with a constant current of 50 mA at room temperature, which is about 2.5 times the value of its nominal operation current (20 mA) for up to 900 ks.

As can be seen from Fig. 1(a) and the inset, the OP decreases dramatically and continuously with no shift of the peak wavelength with the increase in stress time, indicating that a severe damage occurs in the device. In addition, the degradation is more predominant at low input current levels as compared to other regions, which strongly indicates that nonradiative recombination centers are generated.¹¹

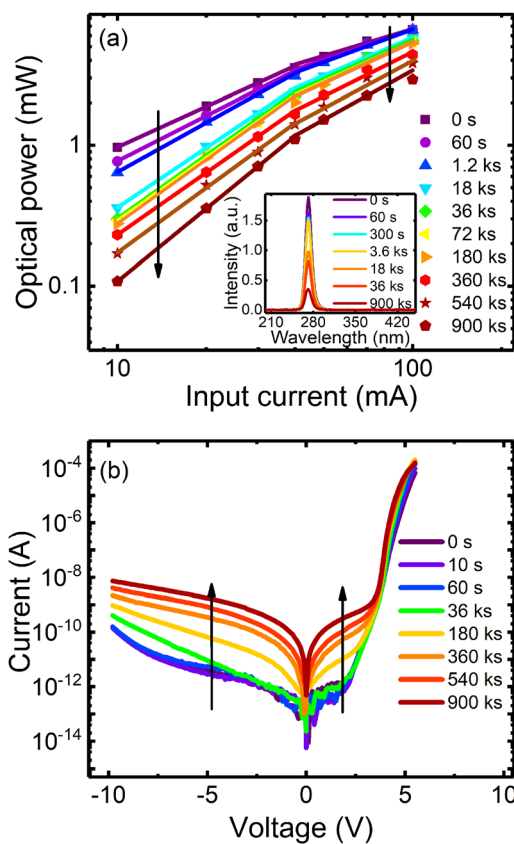


FIG. 1. (a) Optical power vs input current curves of UV-C LED during stress. The duration of the input current is much less than 1 s. Inset: EL spectra measured at 20 mA during stress. (b) Current–voltage (I – V) characteristics of the UV-C LED during stress at room temperature (295 K). The device was stressed with a constant current of 50 mA.

The electrical properties were also described by the I – V characteristic. It can be observed from Fig. 1(b) that the current at both the reverse and low forward bias regions increases under stress. Usually, the reverse leakage current can be attributed to the parasitic leakage paths for carriers, and the forward leakage current can be attributed to the defect-assisted tunneling process.¹⁷ From previous reports, the generation of the nonradiative path was commonly attributed to the generation of defects activated by carrier transport.^{18,19} The parasitic leakage path was typically induced by defects within or around the active region.^{20–22} Therefore, both the optical and electrical degradation can be attributed to the generation of new defects induced by stress.

Due to the irrelevance of injection efficiency—unreachable for electroluminescence—the PL measurement was carried out to identify the newly generated defect.²³ He–Cd laser emitting at 325 nm was applied to the fresh and stressed UV-C LEDs from the n-type region side at room temperature. The beam diameter and the integrated time are $1\text{ }\mu\text{m}$ and 0.5 s, respectively. It can be noticed from Fig. 2 that the peak at 515 nm increases evidently after stress. Moreover, the comparison of images shown in the inset of Fig. 2 signifies the strong intensity of defect excitation in the stressed device. Due to the blue shift of emission in AlGa N ,²⁴ the peak at 515 nm can be attributed to a “yellow luminescence.” Several groups have demonstrated that a yellow luminescence (especially at 2.4 eV) is attributed to transitions involving Ga vacancy (V_{Ga}).^{25–27} Therefore, the newly generated defect can be attributed to V_{Ga} .

In order to have an in-depth investigation on the generated defects, the defect energy level and evolution were then investigated by the DLTS measurement in the following. To probe the Si-doped n-type region (including the active region and the n-AlGa N buffer layer), the DLTS spectra were recorded at a quiescent bias of -6 V with a filling pulse bias and a width of -2 V and 10 ms, respectively. The measurements were carried out in the temperature range between 295 and 80 K with a frequency of 1 MHz. As shown in Fig. 3(a), a positive peak C at about 120 K remains almost constant during stress, corresponding to a carrier freeze-out.²⁸ At 36 ks, a shoulder emerges at 160 K and then grows up to be an obviously positive peak labeled as B. (The same is true for other rate windows, which are not shown here.) Moreover, the increase in peak B is always accompanied by a

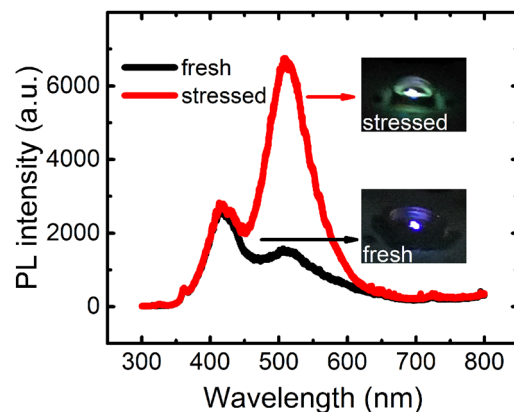


FIG. 2. PL spectra of UV-C LED before and after electrical stress (take 900 ks as an example) at room temperature (295 K). The insets are the image of the fresh and stressed UV-C LEDs during measurement, respectively.

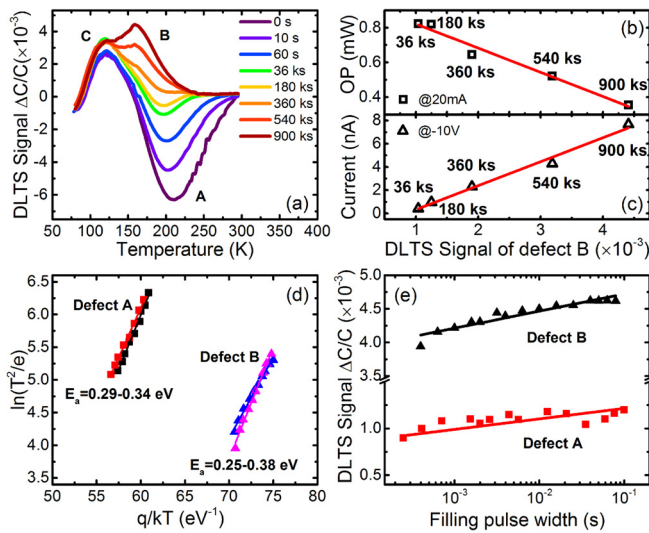


FIG. 3. (a) DLTS spectra of UV-C LED measured under a reverse bias of -6 V, a filling pulse voltage of -2 V, and a pulse width of 10 ms during stress. The rate window is 3.6 ms. In our measurement system, the positive and negative peaks are associated with the majority (electron) and minority (hole) traps, respectively. (b) Correlation between the OP (take the input current of 20 mA as an example) and the DLTS signal of defect B during stress. (c) Correlation between the leakage current (take the reverse bias of -10 V as an example) and the DLTS signal of defect B during stress. (d) Arrhenius plots of defect A (square) and defect B (triangle). (e) Dependence of the DLTS signal on the filling pulse width for defect A and defect B, at the peak temperature. The rate window is 3.6 ms.

reduction of the negative peak A, suggesting the strong correlation between these two defects. The OP and the reverse current during stress were extracted as a function of the DLTS signal of defect B, which are shown in Figs. 3(b) and 3(c), respectively. The good linear relationship demonstrates that the generation/propagation of defect B plays an essential role in the degradation of the optical and electrical characteristics in UV-C LEDs.²⁹

Energy levels and spatial configurations of the defects were additionally obtained from the Arrhenius plot and the dependence of the DLTS signal on the filling pulse width (t_p), respectively. As shown in Fig. 3(d), the energy levels (cross sections) of hole trap A and electron trap B are $0.29\text{--}0.34$ eV (2.51×10^{-16} – 1.87×10^{-15} cm²) and $0.25\text{--}0.38$ eV (8.25×10^{-16} – 1.12×10^{-14} cm²), respectively. The degradation of the AlGaIn-based UV-C LED was usually attributed to the generation of non-interacted point defects. However, point defects can be more interacted at dislocations that are widely distributed in nitride during heteroepitaxy.^{30,31} Therefore, it is significant to reveal whether the defect is point-like or linearly arranged. The relationship between the DLTS signal and t_p is shown in Fig. 3(e). Obviously, the DLTS signals for both defect A and defect B have a logarithmic dependence on t_p . Generally, if the concentration of the occupied defects (n_T), which is proportional to the DLTS signal, depends logarithmically on t_p , the defects are linearly arranged.^{32,33} The dependence can be expressed as

$$n_T(t_p) \propto \tau N_T \ln\left(\frac{t_p}{\tau}\right), \quad (1)$$

where τ is the characteristic time and N_T is the total concentration of trap states.^{34,35} Accordingly, the relationship intuitively indicates the

linear arrangement signature of defects. On the one hand, defect B with the energy level of $0.25\text{--}0.38$ eV corresponds well to V_{Ga} along dislocation,^{36–38} which is also in good agreement with the PL results. On the other hand, since defect A and defect B evolve correlatively during stress and possess similar spatial configurations, the generation of V_{Ga} presents a strong relation to the reduction of defect A.

To further study the process of defect evolution, the atomic concentrations of doping impurities (Si and Mg) and background impurity (O) in fresh UV-C LED are determined using the PCOR-SIMS technique. During the growth process of nitride devices, V_{Ga} usually forms complexes with substitutional O.^{39,40} However, as shown in Fig. 4, the low concentration of O atom in our device indicates that the increase in V_{Ga} after stress is independent of O, which is also in agreement with the PL results. For doping impurities, except for the necessary existence of Si, the concentration of Mg is unusually high in the n-type region. The coexistence of the intentionally doped Si and the unintentionally doped Mg can be attributed to multiple factors. The significantly reduced formation energy of Mg_{Ga} in the n-type region, the diffusion from the p-type region, and the strong memory effect in the MOCVD growth process have been demonstrated.^{26,41,42} Accordingly, the generation of the Ga vacancy can be induced in three ways: the departure of Ga, Si, and Mg atoms from the site of Ga in AlGaIn, respectively.

The generation of Ga vacancy from the departure of Ga, Si, and Mg was then evaluated using the first-principle calculation, respectively. All of the calculations were based on the density functional theory (DFT) carried out by VASP.⁴³ A special quasi-random structure (SQS) method was employed to generate the $Al_{0.5}Ga_{0.5}N$ alloy with 128 atoms,⁴⁴ which corresponds to the bulk of the active region and has been demonstrated to be large enough to describe the defect behaviors.^{45,46} The electron interactions were described by the projected augmented wave method with Perdew–Becke–Ernzerhof as the exchange–correlation energy functional.^{47,48} The energy cutoff is 520 eV, and the atomic structures were relaxed until the force on each atom is below 0.01 eV/Å. Then, the defect evolution was calculated by the dimer methods of the transition state theory.^{49,50} Two critical energies corresponding to the possibility of the defect evolution were determined: the formation energy and the energy barrier, which are

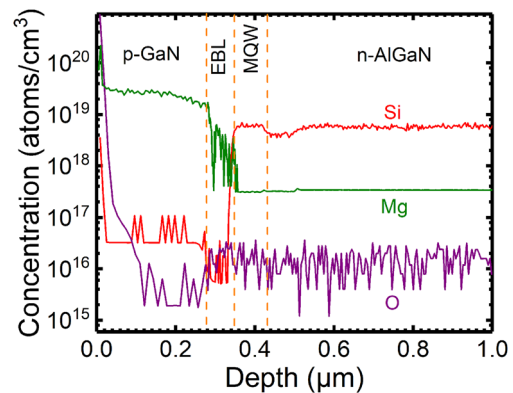


FIG. 4. PCOR-SIMS profile of fresh UV-C LED: doping impurities (Si and Mg) and background impurity (O) are shown. The sample surface is on the left. The detection limits of elements above are below 10^{16} atoms/cm³.

defined as the energy difference between the final and the initial states and the highest energy barrier during defect formation, respectively. In order to achieve a high accuracy of the formation energy and the energy barrier, the energies of all models are obtained by the hybrid functional calculation based on HSE06.⁵¹ As shown in Fig. 5, the departure of Si from Si_{Ga} and the departure of Ga from the Ga site present similarly high energy barrier and formation energy. As it comes to the departure of Mg from Mg_{Ga}, the energy barrier is 25.9% and 26.1% lower than that of Ga and Si, respectively. The formation energy also shows a reduction of 28.4% and 21%, respectively. Accordingly, the departure of Mg from Mg_{Ga} can be much more active as compared to other processes. This process also agrees well with the DLTS results, as the hole trap nature and the energy level of defect A are in good agreement with Mg_{Ga}.⁵² Therefore, the departure of Mg from Mg_{Ga} is demonstrated to be responsible for the generation of V_{Ga} during stress.

In summary, defect behaviors in the degradation of the AlGa_N-based UV-C LEDs under constant current stress are systematically studied. It is found that the degradation is mainly derived from the generation of V_{Ga} in the Si-doped region, as both the reduction of the OP and the increase in the reverse current are well-linearly related to the increase in V_{Ga}. Interestingly, it is observed that the increase in V_{Ga} is always accompanied by a reduction of a hole trap. DLTS signals of two defects mentioned above have a logarithmic dependence on t_p , which demonstrates that both V_{Ga} and the hole trap are arranged along dislocation. Combining the PCOR-SIMS technique with the DFT, the hole trap is identified as Mg_{Ga} along dislocation, based on the relatively high concentration of Mg and the relatively low energy barrier and formation energy of V_{Ga} from Mg_{Ga}. Then, a defect evolution model can be proposed: under electrical stress, the departure of Mg from Mg_{Ga} along dislocation induces the generation of V_{Ga}, which yields a degradation in the AlGa_N-based UV-C LEDs. Since electrical stress is inevitable in the device operation, the study indicates that the dislocation and the unintentionally doped Mg, which commonly exist

in the nitride growth, should be of much concern in the fabrication of UV-C LEDs. This investigation not only reveals new defect behaviors during stress but also opens the way to achieve high reliability AlGa_N-based UV-C LEDs.

This work was supported by the National Natural Science Foundation of China under Grant Nos. 61974115, 61634005, 11690042, 61974111, and 61904142, by the National Pre-research Foundation of China under Grant No. 31512050402, by the Fund of Innovation Center of Radiation Application under Grant No. KFZC2018040202, by the Natural Science Basic Research Plan in Shaanxi Province of China program (No. 2019ZDLGY16-03), and by the Fundamental Research Funds for the Central Universities (No. JB191109).

DATA AVAILABILITY

The data that support the findings of this study are available from the corresponding author upon reasonable request.

REFERENCES

- M. Kneissl, T.-Y. Seong, J. Han, and H. Amano, *Nat. Photonics* **13**, 233 (2019).
- M. S. Shur and R. Gaska, *IEEE Trans. Electron Devices* **57**, 12 (2010).
- C. Chu, K. Tian, Y. Zhang, W. Bi, and Z.-H. Zhang, *Phys. Status Solidi A* **216**, 1800815 (2019).
- S.-I. Inoue, N. Tamari, and M. Taniguchi, *Appl. Phys. Lett.* **110**, 141106 (2017).
- R. G. James, C. Jianfeng, R. G. Shawn, C. M. Mark, G. M. Craig, R. Lee, A. G. Gregory, W. Michael, and J. S. Leo, *Appl. Phys. Express* **6**, 032101 (2013).
- S. Max, S. Wenhong, J. Rakesh, L. Alex, H. Xuhong, D. Alex, B. Yuri, Y. Jinwei, A. G. Gregory, E. R. Lee, W. Michael, S. Michael, and G. Remis, *Semicond. Sci. Technol.* **29**, 084007 (2014).
- S. Max, S. Wenhong, L. Alex, H. Xuhong, D. Alex, B. Yuri, Y. Jinwei, S. Michael, G. Remis, M. Craig, G. Gregory, and W. Michael, *Appl. Phys. Express* **5**, 082101 (2012).
- T. Takayoshi, M. Takuya, S. Jun, N. Norimichi, T. Kenji, and H. Hideki, *Appl. Phys. Express* **10**, 031002 (2017).
- Z.-H. Zhang, J. Kou, S.-W. H. Chen, H. Shao, J. Che, C. Chu, K. Tian, Y. Zhang, W. Bi, and H.-C. Kuo, *Photonics Res.* **7**, B1 (2019).
- C. De Santi, M. Meneghini, D. Monti, J. Glaab, M. Guttman, J. Rass, S. Einfeldt, F. Mehnke, J. Enslin, T. Wernicke, M. Kneissl, G. Meneghesso, and E. Zanoni, *Photonics Res.* **5**, A44 (2017).
- M. Meneghini, L. Trevisanello, G. Meneghesso, and E. Zanoni, *IEEE Trans. Device Mater. Reliab.* **8**, 323 (2008).
- C. G. Moe, M. L. Reed, G. A. Garrett, A. V. Sampath, T. Alexander, H. Shen, M. Wraback, Y. Bilenko, M. Shatalov, J. Yang, W. Sun, J. Deng, and R. Gaska, *Appl. Phys. Lett.* **96**, 213512 (2010).
- J. Glaab, J. Haefke, J. Ruschel, M. Brendel, J. Rass, T. Kolbe, A. Knauer, M. Weyers, S. Einfeldt, M. Guttman, C. Kuhn, J. Enslin, T. Wernicke, and M. Kneissl, *J. Appl. Phys.* **123**, 104502 (2018).
- M. W. Moseley, A. A. Allerman, M. H. Crawford, J. J. Wierer, M. L. Smith, and A. M. Armstrong, *J. Appl. Phys.* **117**, 095301 (2015).
- M. Meneghini, S. Vaccari, N. Trivellin, D. Zhu, C. Humphreys, R. Butendheich, C. Leirer, B. Hahn, G. Meneghesso, and E. Zanoni, *IEEE Trans. Electron Devices* **59**, 1416 (2012).
- L. Huang, T. Yu, Z. Chen, Z. Qin, Z. Yang, and G. Zhang, *J. Lumin.* **129**, 1981 (2009).
- E. Jung, J. K. Lee, M. S. Kim, and H. Kim, *IEEE Trans. Electron Devices* **62**, 3322 (2015).
- F. Rossi, M. Pavesi, M. Meneghini, G. Salviati, M. Manfredi, G. Meneghesso, A. Castaldini, A. Cavallini, L. Rigutti, U. Strass, U. Zehnder, and E. Zanoni, *J. Appl. Phys.* **99**, 053104 (2006).
- M. Meneghini, A. Tazzoli, G. Mura, G. Meneghesso, and E. Zanoni, *IEEE Trans. Electron Devices* **57**, 108 (2010).

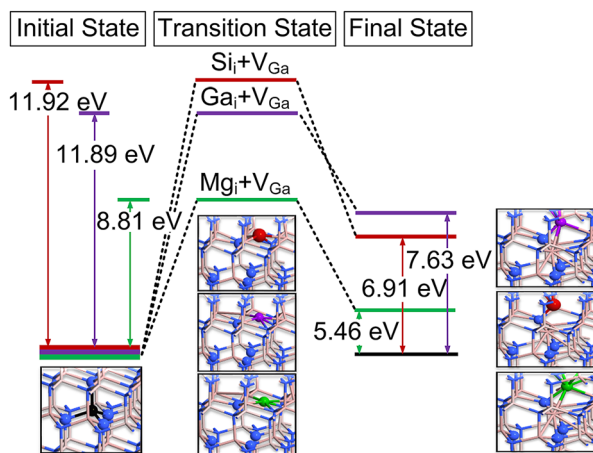


FIG. 5. Energy diagram of the generation of V_{Ga} and snapshots of the atomic structure at the initial, transition, and final states. The green, violet, and red correspond to the departure of Mg, Ga, and Si, respectively. The blue balls are nitrogen atoms at V_{Ga}. The initial state corresponds to the substitution defect (Mg_{Ga} or Si_{Ga}) or the pristine Ga site. The final state corresponds to V_{Ga} with interstitial defects. The transition state denotes the status of the highest energy during defect evolution.

- ²⁰J. Glaab, C. Ploch, R. Kelz, C. Stölmacker, M. Lapeyrade, N. L. Ploch, J. Rass, T. Kolbe, S. Einfeldt, F. Mehnke, C. Kuhn, T. Wernicke, M. Weyers, and M. Kneissl, *MRS Proc.* **1792**, mrss15 (2015).
- ²¹X. A. Cao, P. M. Sandvik, S. F. LeBoeuf, and S. D. Arthur, *Microelectron. Reliab.* **43**, 1987 (2003).
- ²²S. W. Lee, D. C. Oh, H. Goto, J. S. Ha, H. J. Lee, T. Hanada, M. W. Cho, T. Yao, S. K. Hong, H. Y. Lee, S. R. Cho, J. W. Choi, J. H. Choi, J. H. Jang, J. E. Shin, and J. S. Lee, *Appl. Phys. Lett.* **89**, 132117 (2006).
- ²³M. L. Grassa, M. Meneghini, C. De Santi, M. Mandurrino, M. Goano, F. Bertazzi, R. Zeisel, B. Galler, G. Meneghesso, and E. Zanoni, *Microelectron. Reliab.* **55**, 1775 (2015).
- ²⁴M. L. Nakarmi, N. Nepal, J. Y. Lin, and H. X. Jiang, *Appl. Phys. Lett.* **94**, 091903 (2009).
- ²⁵A. Y. Polyakov and I.-H. Lee, *Mater. Sci. Eng. R* **94**, 1 (2015).
- ²⁶M. A. Reshchikov and H. Morkoç, *J. Appl. Phys.* **97**, 061301 (2005).
- ²⁷M. Meneghini, D. Barbisan, L. Rodighiero, G. Meneghesso, and E. Zanoni, *Appl. Phys. Lett.* **97**, 143506 (2010).
- ²⁸A. Castaldini, A. Cavallini, L. Rigutti, M. Meneghini, S. Levada, G. Meneghesso, E. Zanoni, V. Härle, T. Zahner, and U. Zehnder, *Phys. Status Solidi C* **2**, 2862 (2005).
- ²⁹D. Monti, M. Meneghini, C. D. Santi, G. Meneghesso, E. Zanoni, J. Glaab, J. Rass, S. Einfeldt, F. Mehnke, J. Enslin, T. Wernicke, and M. Kneissl, *IEEE Trans. Electron Devices* **64**, 200 (2017).
- ³⁰X. H. Wu, P. Fini, E. J. Tarsa, B. Heying, S. Keller, U. K. Mishra, S. P. DenBaars, and J. S. Speck, *J. Cryst. Growth* **189–190**, 231 (1998).
- ³¹Y. Tokuda, Y. Matuoka, K. Yoshida, H. Ueda, O. Ishiguro, N. Soejima, and T. Kachi, *Phys. Status Solidi C* **4**, 2568 (2007).
- ³²M. Meneghini, M. la Grassa, S. Vaccari, B. Galler, R. Zeisel, P. Drechsel, B. Hahn, G. Meneghesso, and E. Zanoni, *Appl. Phys. Lett.* **104**, 113505 (2014).
- ³³G. Venturi, A. Castaldini, A. Cavallini, M. Meneghini, E. Zanoni, D. Zhu, and C. Humphreys, *Appl. Phys. Lett.* **104**, 211102 (2014).
- ³⁴P. Omling, E. R. Weber, L. Montelius, H. Alexander, and J. Michel, *Phys. Rev. B* **32**, 6571 (1985).
- ³⁵A. Hierro, A. R. Arehart, B. Heying, M. Hansen, J. S. Speck, U. K. Mishra, S. P. DenBaars, and S. A. Ringel, *Phys. Status Solidi B* **228**, 309 (2001).
- ³⁶A. F. Wright and U. Grossner, *Appl. Phys. Lett.* **73**, 2751 (1998).
- ³⁷S. M. Lee, M. A. Belkhir, X. Y. Zhu, Y. H. Lee, Y. G. Hwang, and T. Frauenheim, *Phys. Rev. B* **61**, 16033 (2000).
- ³⁸M. A. Reshchikov, H. Morkoç, S. S. Park, and K. Y. Lee, *Appl. Phys. Lett.* **78**, 3041 (2001).
- ³⁹A. Kakanakova-Georgieva, D. Nilsson, X. T. Trinh, U. Forsberg, N. T. Son, and E. Janzén, *Appl. Phys. Lett.* **102**, 132113 (2013).
- ⁴⁰J. Chen, Y. S. Puzyrev, R. Jiang, E. X. Zhang, M. W. McCurdy, D. M. Fleetwood, R. D. Schrimpf, S. T. Pantelides, A. R. Arehart, S. A. Ringel, P. Saunier, and C. Lee, *IEEE Trans. Nucl. Sci.* **62**, 2423 (2015).
- ⁴¹S.-N. Lee, H. S. Paek, J. K. Son, H. Kim, K. K. Kim, K. H. Ha, O. H. Nam, and Y. Park, *J. Electroceram.* **23**, 406 (2009).
- ⁴²Y. Ohba and A. Hatano, *J. Cryst. Growth* **145**, 214 (1994).
- ⁴³G. Kresse and J. Furthmüller, *Phys. Rev. B* **54**, 11169 (1996).
- ⁴⁴A. Zunger, S. H. Wei, L. G. Ferreira, and J. E. Bernard, *Phys. Rev. Lett.* **65**, 353 (1990).
- ⁴⁵S. Wu, X. Yang, H. Zhang, L. Shi, Q. Zhang, Q. Shang, Z. Qi, Y. Xu, J. Zhang, N. Tang, X. Wang, W. Ge, K. Xu, and B. Shen, *Phys. Rev. Lett.* **121**, 145505 (2018).
- ⁴⁶F. Gao, E. J. Bylaska, and W. J. Weber, *Phys. Rev. B* **70**, 245208 (2004).
- ⁴⁷P. E. Blöchl, *Phys. Rev. B* **50**, 17953 (1994).
- ⁴⁸J. P. Perdew, K. Burke, and M. Ernzerhof, *Phys. Rev. Lett.* **77**, 3865 (1996).
- ⁴⁹G. Henkelman and H. Jónsson, *J. Chem. Phys.* **111**, 7010 (1999).
- ⁵⁰A. Heyden, A. T. Bell, and F. J. Keil, *J. Chem. Phys.* **123**, 224101 (2005).
- ⁵¹J. Heyd, G. E. Scuseria, and M. Ernzerhof, *J. Chem. Phys.* **118**, 8207 (2003).
- ⁵²C. G. Van de Walle and J. Neugebauer, *J. Appl. Phys.* **95**, 3851 (2004).